IEEE Access
Multidisciplinary ⋮ Rapid Review ⋮ Open Access Journal

Received 29 September 2023, accepted 30 October 2023, date of publication 24 November 2023,
date of current version 5 December 2023.

Digital Object Identifier 10.1109/ACCESS.2023.3336686

RESEARCH ARTICLE

Adaptive RRI Selection Algorithms for Improved Cooperative Awareness in Decentralized NR-V2X

AVIK DAYAL [1], (Member, IEEE), VIJAY K. SHAH [2], (Member, IEEE), HARPREET S. DHILLON [3], (Fellow, IEEE), AND JEFFREY H. REED [3], (Life Fellow, IEEE)

[1]Johns Hopkins University Applied Physics Laboratory, Laurel, MD 20723, USA
[2]Cybersecurity Engineering Department, George Mason University, Fairfax, VA 22030, USA
[3]Wireless@VT, Bradley Department of ECE, Virginia Tech, Blacksburg, VA 24061, USA

Corresponding author: Avik Dayal (ad6db@vt.edu)

This work was supported in part by the Office of Naval Research (ONR) under Multidisciplinary University Research Initiatives (MURI) Grant N00014-19-1-12621, and in part by Virginia Commonwealth Cyber Initiative (CCI), an Investment by the Commonwealth of Virginia in the Advancement of Cyber Research and Development, Innovation, and Workforce Development.

ABSTRACT Decentralized vehicle-to-everything (V2X) networks (i.e., C-V2X Mode-4 and NR-V2X Mode-2) utilize sensing-based semi-persistent scheduling (SPS) where vehicles sense and reserve suitable radio resources for Basic Safety Message (BSM) transmissions at prespecified periodic intervals termed as *Resource Reservation Interval* (RRI). Vehicles rely on these received periodic BSMs to localize nearby (transmitting) vehicles and infrastructure, referred to as *cooperative awareness*. Cooperative awareness enables line of sight and non-line of sight localization, extending a vehicle's sensing and perception range. In this work, we first show that under high vehicle density scenarios, existing SPS (with prespecified RRIs) suffer from poor cooperative awareness, quantified as *tracking error*. Tracking error is defined as the difference between a vehicle's true and estimated location as measured by its neighbors. To address the issues of static RRI SPS and improve cooperative awareness, we propose two novel *RRI* selection algorithms – namely, *Channel-aware RRI* (Ch-RRI) selection and *Age of Information (AoI)-aware RRI* (AoI-RRI) selection. Ch-RRI dynamically selects an RRI based on *channel resource availability* depending upon the (sparse or dense) vehicle densities, whereas AoI-RRI utilizes a novel information freshness metric, called Age of Information (AoI) to select a suitable RRI. Both adaptive RRI algorithms use SPS for selecting transmission opportunities for timely BSM transmissions at the chosen RRI. System-level simulations demonstrate that both proposed schemes outperform the SPS with fixed RRI in terms of improved cooperative awareness. Furthermore, AoI-RRI SPS outperforms Ch-RRI SPS in high densities, whereas Ch-RRI SPS is slightly better than AoI-RRI SPS in low densities.

INDEX TERMS Age-of-information, dynamic spectrum access, NR-V2X, NR-V2X Mode-2, radio resource management.

I. INTRODUCTION

Modern vehicles have been equipped with a plethora of sensors to assist with autonomous capabilities [1]. The drawback is that most sensors, including cameras, radars, and LIDAR, are limited to line of sight (LOS) visibility and are constrained in their scope [2]. This LOS constraint is a major motivation for the development of Vehicle-to-Everything (V2X) communications. V2X communications enables both LOS and NLOS exchange of sensor data with neighboring vehicles, thereby increasing the range of a vehicle's *awareness* of surrounding vehicles and infrastructure [3].

The Third Generation Partnership Project (3GPP) Release 16 has introduced a V2X communications technology that uses the 5G New Radio (NR) air interface, referred to as 5G NR-V2X. NR-V2X includes enhancements to the 3GPP's previous cellular V2X communications technology (C-V2X) based on the Long-Term Evolution (LTE) standard. NR-V2X offers two modes of operation, termed Mode-1 and Mode-2, that use sidelink communications, which is direct communication between users or vehicles without

The associate editor coordinating the review of this manuscript and approving it for publication was Nitin Gupta.

data passing through the gNodeB [4]. NR-V2X Mode-1 employs a centralized scheduling approach, where a gNodeB schedules and assigns sidelink radio resources for two or more vehicles to communicate and exchange data directly. NR-V2X Mode-2 assumes communications to occur outside the coverage of an gNodeB; therefore, every vehicle uses a sensing-based semi-persistent scheduling (SPS) protocol to sense and reserve sidelink radio resources. SPS was introduced as part of the Release 14 C-V2X Mode-4 standard, the predecessor to NR-V2X Mode-2 [5]. Since cellular connectivity can not be assumed ubiquitous, NR-V2X Mode-2 is considered as the baseline mode for NR-V2X.

In NR-V2X Mode-2 SPS, vehicles sense and select suitable (available) radio resources to transmit packets at predefined fixed time intervals, termed, Resource Reservation Interval (RRI). Equivalently, RRI is defined as the inter-transmission time interval between two consecutive transmissions. In the Release 14 C-V2X standard, RRIs equal to or below 100 ms were restricted to 20 ms, 50 ms, or 100 ms [6]. Release 16 NR-V2X Mode-2 provides more flexibility by allowing any integer RRI between 1 and 99 ms for any RRIs below 100 ms [7].

The primary use case for NR-V2X Mode-2 SPS is the dissemination of basic safety messages (BSMs), which carry time-sensitive state information such as a transmitting vehicle's speed, heading, and location [8]. Receiving vehicles can use these BSMs for *cooperative awareness*, including the localization and trajectory prediction of neighboring vehicles and infrastructure. Cooperative awareness can enable safety-critical applications such as forward collision warnings [9], blind spot/lane change warnings [10], and is likely one of the key requirements for autonomous driving [11]. One metric that can quantify cooperative awareness performance is tracking error, the difference between a vehicle's actual and estimate location (via most recent BSM) by its neighboring vehicles. Tracking error, as opposed to conventional communication metrics such as packet delivery ratio (PDR) and throughput, captures the impact of multiple lost or outdated BSMs on a vehicle's awareness and is thus a more appropriate performance measure for this application.

Since BSMs carry time-sensitive information, outdated BSMs (due to large RRIs) and/or lost BSMs (due to channel congestion) negatively impact the performance of cooperative awareness applications, mainly due to erroneous localization of neighboring vehicles. Therefore, it is critical that the state information in each vehicles transmission be *fresh*, as stale information can compromise the aggregate awareness of the vehicular network. The *freshness* of information at receiving vehicles can be measured using Age-of-Information (AoI). AoI is the time elapsed since new state information has been generated and is a promising metric to measure the freshness of system state information. Results in [12] have found that AoI has a strong correlation with tracking error in vehicular networks, which motivates further study of AoI.

In this work, we explore the deficiencies of the NR-V2X Mode-2 SPS using static RRIs in terms of tracking error and propose algorithms that choose adaptive RRIs to improve the overall cooperative awareness performance of NR-V2X Mode-2. We show in this paper that SPS with static RRIs (e.g. 50 and 100 ms) has cooperative awareness limitations in NR-V2X networks. Consider these scenarios: (i) *high vehicle density scenarios* – the NR-V2X network performance suffers from congestion with a large number of lost packets, leading to an increased tracking error, and (ii) *low vehicle density* – the spectrum resources would be under-utilized in time. The tracking error performance in low density scenarios can improve with a smaller RRI, which ensures frequent location updates without fear of channel congestion. We introduce two adaptive RRI algorithms, termed Channel-aware RRI (Ch-RRI) selection and AoI-aware RRI (AoI-RRI) selection. Ch-RRI uses channel occupancy measurements to find the smallest RRI possible without increasing congestion. Motivated by the benefits of reducing AoI, we propose AoI-RRI, an AoI-aware RRI selection algorithm for NR-V2X Mode-2 that uses the average AoI observed by neighboring vehicles to select an optimal RRI.

In this work, we make following key contributions:

- We show that NR-V2X Mode-2 SPS with static RRIs suffers severely from under- and over-provisioning of radio resources (depending upon the vehicle densities). This in turn negatively impacts the timely successful delivery of BSMs and compromises the cooperative awareness of NR-V2X Mode-2 SPS.
- To address the limitations of SPS with static RRIs, we propose Ch-RRI SPS, which is SPS powered by a *channel aware* RRI selection algorithm. The Ch-RRI algorithm uses channel occupancy measurements and chooses the minimum possible RRI spacing between transmissions without increasing packet loss due to congestion. Ch-RRI SPS uses this RRI spacing to select radio resources for BSM transmissions.
- In a similar vein to Ch-RRI SPS, we develop AoI-RRI SPS, SPS powered by a *AoI aware* RRI selection algorithm. The AoI-RRI algorithm uses neighborhood age and channel resource measurements to choose an age optimal RRI iteratively. To the best of our knowledge, this is the first work that proposes using AoI measurements directly in choosing the optimal RRI spacing in an adaptive manner.
- Experiments developed on our NR-V2X simulator show that when compared to NR-V2X Mode-2 SPS with 20 ms, 50 ms, and 100 ms RRI, the proposed Ch-RRI and AoI-RRI SPS demonstrate a substantial reduction of tracking error. Ch-RRI as compared to AoI-RRI shows a lower AoI and tracking error in low density highway scenarios, and is faster in converging to a local minimum AoI. However, the average AoI and tracking error of AoI-RRI is lower at higher densities.

An earlier version of this paper was presented in part at the 2021 IFIP Networking Conference [13]. A preliminary version of this work appears as a chapter in Avik Dayal's Ph.D. Thesis [14]. The organization of this paper is as follows: Section II discusses related works. Section III discusses cooperative awareness, the tracking error metric, and the NR-V2X Mode-2 standard. In Section IV we illustrate the limitations of traditional fixed RRI SPS and present the algorithmic details of Ch-RRI SPS. Section V provides a brief description of AoI, and discusses the details of AoI-RRI SPS. Finally, Section VI discusses the results and provides an outlook for future work, followed by concluding remarks in Section VII.

II. STATE-OF-THE-ART

There has been a surge of research in the area of simulating and enhancing SPS for C-V2X Mode-4 [6], [15], [16], [17], [18], [19], [20], [21], [22] and more recently, for NR-V2X Mode-2 SPS [23], [24], [25], [26]. The research performed in [15] simulated and provided a baseline for semi-persistent scheduling across various densities for highway and urban environments. Research in [5], [16], and [17] varied the probability of reselection, selection window, and RRI in SPS and measured the impact on the packet delivery ratio (PDR). The authors of [18] concluded that using short term sensing before resource selection reduced packet collisions and improved SPS performance. The work in [19] and [27] was amongst the first to adjust the transmission power and RRI accordingly, to improve the overall performance of SPS. To address the scheduling overhead of SPS, [21] has proposed using single shot transmissions as part of SPS for safety critical messages that have an immediate scheduling need. Although much of the research for semi-persistent scheduling is simulation driven, [22] has provided an analytical model for semi-persistent scheduling in vehicular networks. Recently, the work in [23], [24], [25], and [26] has simulated the relatively new NR-V2X Mode-2 SPS, specifically looking at the impact of the flexible numerology on SPS. A potential drawback of these works is the focus on improving the coverage (typically measured through PDR) of C-V2X Mode-4 and NR-V2X Mode-2, and ignoring the cooperative awareness performance of the vehicular network.

AoI has recently emerged as a popular metric for quantifying the performance of scheduling and decentralized radio resource management in vehicular networks. In particular, there has been a lot of research done in optimizing the broadcast rate to reduce the AoI in networks that use Dedicated Short Range Communications (DSRC), a competing V2X technology based on the 802.11p standard [28], [29], [30], [31], [32], [33], [34]. Although there are notable differences between the two standards, changing the broadcast rate can be seen as the analogous equivalent to using the RRI to minimize the AoI, and merits discussion. The authors in [28] developed a decentralized algorithm that iterated the broadcast rate based on AoI measurements for a DSRC network. The work in [29] proposed a model that uses a vehicular network's connectivity graph to show the relationship between the average system AoI and vehicle density and broadcast intervals. AoI was used to evaluate platooning applications for convoys of vehicles in [30] and [31]. Furthermore, [33] and [34] investigated the effect of the backoff window size in CSMA on the AoI.

Although the SPS protocol in C-V2X Mode-4 and NR-V2X Mode-2 is relatively new, there has been some recent work in applying AoI to SPS. The authors in [20] analyzed the AoI of Release 14 C-V2X Mode-4 and proposed a piggyback collaboration method to help decrease half duplex errors, thereby reducing the AoI. More recently, [35] and [36] looked at the effect of RRI spacing and persistence, respectively, on AoI performance in the NR-V2X Mode-2 standard, and found optimal RRI and persistence values across vehicle densities. Note that although the Release 14 C-V2X Mode-4 SPS is similar to Release 16 NR-V2X Mode-2 SPS, there are a few key differences between the two standards. Two differences that are particularly relevant to this work are the change in ranking of slot resources (discussed in Section IV) and the inclusion of any integer RRI between 1 and 99 ms.[1] These changes can enable higher transmission rates while preventing collisions from choosing the same slot resource [24]. While there have been recent works evaluating the overall performance of Release 16 NR-V2X SPS, to the best of our knowledge, this is the first work that evaluates the AoI and cooperative awareness performance for NR-V2X SPS and the first work to directly use AoI measurements to optimize the RRI for SPS.

III. COOPERATIVE AWARENESS AND NR-V2X MODE-2

This section discusses cooperative awareness, the tracking error metric, and the NR-V2X Mode-2 standard for sidelink communications from the physical layer structure to the semi-persistent scheduling algorithm that vehicles use to find and reserve suitable transmission opportunities.

A. COOPERATIVE AWARENESS AND TRACKING ERROR

Since cooperative awareness depends on the sharing of time-sensitive information with other vehicles via BSMs, conventional communication metrics such as latency, throughput, and packet delivery ratio (PDR) greatly impact a vehicle's awareness. However, these metrics alone cannot capture the impact of multiple lost or outdated BSMs on a vehicle's awareness, as illustrated by the following example. Consider a fast moving vehicle travelling at 140 km/hr (38.89 m/s) while transmitting with a high RRI (100 ms or more). Neighboring vehicles receive location packets reliably, but because there is at least 100 ms between packets, the localization or *tracking* error would be at least 3.89 m. Likewise, a low RRI (50 ms or less) would yield a tracking error of at least 1.94 m, though this tracking error could

[1]Please refer to [7] for a detailed discussion on the differences between C-V2X Mode-4 and NR-V2X Mode-2.

increase if packets are dropped due to channel congestion. Thus, as the above example shows, a tracking error metric can provide a better context to the cooperative awareness performance in vehicular networks.

Illustrated in Fig. 1, tracking error (e_{uv}^{track}) in the context of NR-V2X is defined as the difference in the transmitting vehicle's (vehicle u) true location, and u's estimated location by neighboring receiving vehicle v. We assume that the receiving vehicle v is transmission range of u and time t' is the generation time of the transmission from u to v. The tracking error is calculated as:

$$e_{uv}^{track} = \sqrt{(x_u^t - \hat{x}_{uv})^2 + (y_u^t - \hat{y}_{uv})^2}, \quad (1)$$

where (x_u^t, y_u^t) is u's true current 2-D location at time t and $(\hat{x}_{uv}, \hat{y}_{uv})$ is u's previous location from time t' at vehicle v from the last transmission received from u.

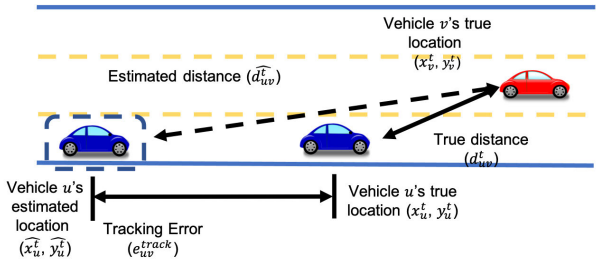

FIGURE 1. Illustration of latency induced tracking error in a vehicular network.

The tracking error has a large impact on the cooperative awareness in vehicular networks because

1) The RRI (or inter-packet transmission interval) can cause a large tracking error, especially at higher speeds.
2) Channel congestion could lead to several lost and delayed packets, further deteriorating tracking error. In the example of a vehicle traveling at 140 km/hr with a 50 ms RRI in a congested environment, two consecutive missed packets could cause a 5.833 m tracking error.

A lower tracking error at receiving vehicle v implies that v can accurately position (or *localize*) u. Note from the above discussion that a lower RRI can decrease the tracking error but can also increase the number of lost packets due to channel congestion.

B. PHYSICAL LAYER STRUCTURE FOR THE NR-V2X SIDELINK

Rel. 16 NR-V2X sidelink is designed to operate in two different frequency ranges, from 0.410- 7.125 GHz (FR1) and 24.25- 52.5 GHz (FR2) [7]. Though both frequency ranges are supported in Rel. 16, NR-V2X is expected to operate in the FR1. The NR-V2X sidelink uses cylic prefix orthogonal frequency modulation (CP-OFDM) and supports multiple subcarrier spacings of 15, 30, and 60 kHz.

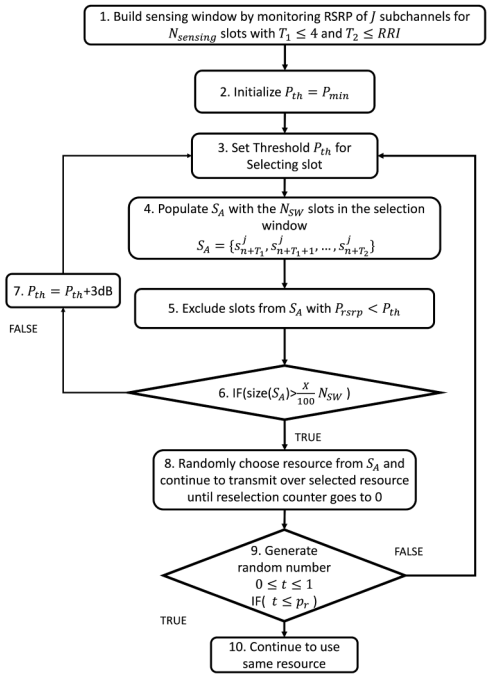

FIGURE 2. Flowchart of SPS Algorithm.

1) RESOURCE STRUCTURE IN TIME DOMAIN

In the NR-V2X sidelink, resources in the time domain are made up of frames, subframes, and slots. Every frame is made up of 10 subframes, and each frame time length is typically 10 ms [4]. Subframes are typically 1 ms in length, and broken down into slots. A slot consists of 4 OFDM symbols, which means that the length of each slot depends on the chosen subcarrier spacing. A subcarrier spacing of 15 kHz corresponds to a slot length of 1 ms, while a 60 kHz subcarrier spacing corresponds to a 0.25 ms length [37]. For the purposes of the work, we assume NR-V2X Mode-2 SPS is inter-operable with C-V2X Mode-4, and take assume a subcarrier spacing of 15 KHz

2) RESOURCE STRUCTURE IN FREQUENCY DOMAIN

The smallest schedulable unit of frequency are resource blocks (RB). In the 5G NR standard, a RB is made up of 12 equally spaced subcarriers. The bandwidth of each RB depends on the subcarrier spacing value. RBs are combined sequentially to form subchannels. In NR-V2X, the data packets, or Transport Blocks, are transmitted on one or more subchannels. In each subframe, alongside every TB, is a sidelink control information block with modulation and coding scheme used [5].

C. NR-V2X MODE-2 SEMI-PERSISTENT SCHEDULING

At the MAC layer, the NR-V2X sidelink utilizes semi-persistent scheduling (SPS) that uses sensing to determine suitable semi-persistent transmission opportunities, i.e., set of slots, for BSM transmission. Fig. 2 depicts the SPS algorithm,[2] and is explained below. We use s_i^j to refer to

[2]Please refer to [6] and [7] for a detailed discussion on NR-V2X and SPS.

a single-slot resource where i is the slot index and j is the subchannel index of J total subchannels.

- **Sensing (Step 1):** Each vehicle continuously monitors the slots by measuring the reference signal received power (RSRP) across all J subchannels; and stores sensing measurements for a prespecified last $N_{sensing}$ slots, known as the *sensing window*. Let slot s_n denote the first slot after the sensing window. Then we can write the sensing window at s_n as the following set of single-slot resources for the j^{th} subchannel: $\left[s^j_{n-N_{sensing}}, \ldots, s^j_{n-1}\right]$.
- **Identifying Available Resources (Steps 1-8):** Each vehicle initializes a *selection window* with a set of consecutive candidate slots (See Step 1). $T_1 \leq 4$ and $T_2 \leq RRI$ are the start and end slots for the selection window. The **RRI** refers to the time interval between two consecutive BSM transmissions.[3] Each vehicle utilizes $N_{sensing}$ slots (obtained in Step 1) for identifying and subsequently, selecting the available slot within the selection window for BSM transmission as follows.
  1) The vehicle sets – (i) the RSRP threshold, P_{th}, to a minimum RSRP value, P_{min} (Steps 2-3) and (ii) initializes set S_A as all slots in the selection window, i.e., $S_A = [s_{n+T_1}, s_{n+T_1+1}, \cdots, s_{n+T_2}]$ (See Step 4).
  2) As shown in Step 5 of Fig. 2, the vehicle excludes all candidate subframes from set S_A if one of the following conditions are met – (i) the vehicle has not monitored the corresponding candidate subframe in the sensing window (i.e., $N_{sensing}$) due to the half duplex exclusion criteria and (ii) the RSRP measurement for corresponding candidate subframe is higher than P_{th}. The RSRP exclusion criteria for the i^{th} subframe (for jth sub-channel) in the selection window can be written as
  $$RSRP\left(s^j_{n+T_1+i-N_{sensing}}\right) \geq P_{th} \quad (2)$$
  3) If the remaining slots in S_A is less than $X\%$ of the total available slots (Step 6), then P_{th} is increased by 3 dB (Step 7), and Steps 3 to 5 are repeated. In NR-V2X Mode-2, X can be set to 20, 35 or 50.
  4) Each vehicle selects a random slot resource from the resources remaining in S_A for transmission in Step 7.[4]
- **Resource Reselection (Steps 8-10):** Each vehicle can reserve the same slot (selected in Step 7) for next *Resource Counter (RC)*[5] number of subsequent transmissions with the same transmission interval, i.e., *RRI*. The RC varies with the RRI to ensure that the selected slot/resource is in use for at least 0.5 s and at most 1.5 s. This means that for a 20 ms RRI, $25 \leq$ RC ≤ 75, for 50 ms RRI, $10 \leq$ RC ≤ 30, and for a 100 ms RRI, $5 \leq$ RC ≤ 15.
  After RC reaches 0, the vehicle can either continue utilizing the preselected resources with a probability p_r or reselect new resources for BSM transmissions with a probability $(1 - p_r)$ (See Steps 8-9).

[3]In NR-V2X Mode-2 SPS, each vehicle selects an RRI at the time of resource selection, although the standard leaves the selection of RRI up to the user [7].

[4]Note that Release 14 SPS had an additional selection criteria that selected slot resources with the lowest sidelink received strength indicator (S-RSSI) measurements. This was removed in Release 16 to accommodate smaller RRIs [24].

[5]Resource Counter (RC) is the maximum number of transmissions a certain vehicle is allowed (by utilizing the selected slot/resource in the current selection window) before having to reselect a new set of resources.

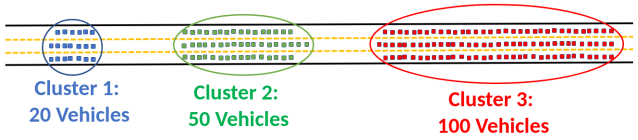

FIGURE 3. NR-V2X example network with three clusters of vehicles.

IV. CH-RRI SPS: SEMI-PERSISTENT SCHEDULING USING CHANNEL AWARE RRI SELECTION

In this section, we present the limitations of conventional SPS protocol in terms of improving cooperative awareness performance of NR-V2X Mode-2, followed by detailed discussion on how to overcome them through a novel channel aware RRI selection algorithm (Ch-RRI SPS). The Ch-RRI SPS discussion first formulates the channel aware RRI selection problem as an Integer Linear Programming (ILP) problem and then goes into the algorithmic details of the proposed Ch-RRI SPS protocol.

A. LIMITATIONS OF SPS ON COOPERATIVE AWARENESS

We present the limitations of SPS through a simple NR-V2X example (See Fig. 3). The example NR-V2X network consists of three clusters,[6] of vehicles, where clusters 1, 2, and 3 respectively have 20, 50, and 100 vehicles. We make the following **assumptions** for all example NR-V2X scenarios.

- We assume $T_1 = 0$ and $T_2 =$ RRI, which means, the size of selection window is equal to the RRI.
- The NR-V2X physical layer consists of 2 subchannels only. Each BSM transmission uses both the subchannels and takes 1 ms to transmit. This means if the selection window is 100 ms (i.e., RRI = 100 ms), then at most 100 distinct vehicles have unique BSM transmission opportunities (assuming no collision in resource selection).
- Each cluster of vehicles is sufficiently spaced apart from each other so that there is no inter-cluster interference. This means, for example, no transmissions from cluster 2 interfere with any transmissions from cluster 1, and vice-versa.

Under the above assumptions, let us look at the (i) *Channel Occupancy Percentage* $C^{(i)}_{occup}$, defined as the percentage of the number of vehicles transmitting to the total number of available slots transmission opportunities for the i^{th} cluster,

[6]Each vehicle is at 1-hop (i.e., within the transmission range) of every other vehicles belonging to a certain cluster of vehicle.

TABLE 1. Ideal Channel Occupancy Percentage and Success Probability of Conventional SPS with Fixed RRIs vs Scheduling with Adaptive RRI.

Metrics	Conventional SPS			**Ch-RRI**
	20 ms	50 ms	100 ms	**Adaptive RRI**
Channel Occupancy Percentage	379.4%	152.94%	75.88%	100%
Probability of Successful Reception	0.35	0.7058	1	1

and (ii) *Probability of Successful Reception* (P_{suc}). For simplicity, let P_{suc} is given by $\frac{1}{N}$ where N is the number of vehicles using the same slot for BSM transmissions. Note that we only make this P_{suc} assumption here to simplify this discussion on the limitations of fixed RRI SPS. In simulations and reality, P_{suc} gets worse as N increases.

Table 1 depicts the average $C^{(i)}_{occup}$ and P_{suc} observed in the example ideal NR-V2X network (meaning slot resources are distributed evenly across all vehicles) under conventional SPS with three different values of RRIs, i.e., 20 ms, 50 ms, and 100 ms. For instance, the average $C^{(i)}_{occup}$ for SPS with low RRI = 20 ms is given by $\frac{\sum RRI \times (C^{(i)}_{occup}}{\text{total number of vehicles}}$. $C^{(i)}_{occup}$ for each cluster can be computed as follows: Since RRI is 20 ms, there are 20 transmission opportunities (or slots), (i) in cluster 1, 20 vehicles attempt to transmit, which implies $C^{(1)}_{occup} = \frac{20}{20} \times 100 = 100\%$, (ii) in cluster 2, 50 vehicles attempt to transmit, which results in $C^{(2)}_{occup} = \frac{50}{20} \times 100 = 250\%$, and (iii) in cluster 3, 100 vehicles attempt to transmit, resulting in $C^{(3)}_{occup} = 500\%$. Thus, the average C_{occup} is $\frac{20\times C^{(1)}_{occup}+50\times C^{(2)}_{occup}+100\times C^{(3)}_{occup}}{20+50+100} \times 100 = 379.4\%$. The average P_{suc} can be computed in the similar fashion, and it turns out to be 0.35 in case of SPS with RRI as 20 ms. On contrary for SPS with high RRI = 100 ms the average C_{occup} and P_{suc} are 75.88% and 1 respectively.

Note that SPS with low RRI such as, 20 ms leads to *overly congested radio channels* (379.4%), and thus, large number of dropped BSM packets (0.35), particularly, in clusters 2 and 3 with $>$ 20 vehicles). The lost packets result in high tracking error, which compromises the awareness of considered NR-V2X network. Whereas, in case of SPS with high RRI as 100 ms, the radio resources are under-utilized (75%), particularly in cluster 1 and 2 with $<$ 100 vehicles. Tracking error performance can be significantly improved by choosing lower value of RRI as lower value of RRIs will improve timely delivery of BSMs. From the above discussion, it is evident that SPS with fixed RRI (irrespective of the chosen value of RRI) is limited in the context of improving overall cooperative awareness of NR-V2X networks.

To better address the limitations of static RRI SPS, we propose Ch-RRI, an adaptive RRI selection algorithm where each vehicle chooses its RRI based on the neighborhood density. Ideally, in the example NR-V2X network depicted in Fig. 3, Ch-RRI would choose RRI = 20 ms for a vehicle in cluster 1 (with 20 vehicles). Similarly, Ch-RRI will choose RRI = 50 ms for cluster 2 (with 50 vehicles) and RRI = 100 ms for cluster 3 (with 100 vehicles) – which will result in $C_{occup} = 100\%$ and $P_s = 1$ (See Table 1). It means that the proposed Ch-RRI strategy with adaptive RRI enables judicious utilization of the radio resources. This in turn reduces the tracking error and enhances the cooperative awareness of NR-V2X networks.

B. PROBLEM FORMULATION

1) NOTATIONS

At each time instant $t \in T$, let $s(t, P_{th})$ denote the set of available slots (slots with observed power less than P_{th}) in the neighborhood of any vehicle v. RRI_v is the v^{th} vehicle's RRI and $\mathcal{N}$ is the set of all vehicles in the environment.

2) OBJECTIVE FUNCTION

As shown in Eq. 3, the objective function is to minimize the resource reservation interval (RRI) (or maximize BSM rate) at each vehicle v (where $v \in \mathcal{N}$) over the entire time duration T.

$$\min \sum_{t\in T} \frac{1}{|\mathcal{N}|} \sum_{v\in\mathcal{N}} \text{RRI}_v(t) \tag{3}$$

$$\text{subject to} \sum_{v\in\mathcal{N}} \text{RRI}_v(t) \leq s(t, P_{th}), \forall v \in \mathcal{N}, t \in T \tag{4}$$

$$\text{RRI}_{min} \leq \text{RRI}_v(t) \leq \text{RRI}_{max}, \forall v \in \mathcal{N}, t \in T \tag{5}$$

3) CONSTRAINTS

Eq. 4 constrains that the sum total of the RRI interval must be less than the number of slots available to each vehicle v at time instant t. This constraint ensures that the channel congestion or the outage probability across all vehicles are not compromised. Eq. 5 restricts the RRI for each vehicle to be within the range $[\text{RRI}_{min}, \text{RRI}_{max}]$.

Note that solving the aforestated ILP formulation would provide the optimal solution to Ch-RRI. However, this is impractical in a real-world NR-V2X setting because of the dynamic nature of the setup (mobility of vehicles) and lack of global knowledge. Additionally, in order to solve the ILP problem, we would require the knowledge of available slots at future time instants, which is impractical to obtain in time varying NR-V2X networks. Therefore, our proposed Ch-RRI SPS is based on decentralized SPS and estimates the latest channel occupancy (via sensing window), selecting the suitable value of RRI at each vehicle in the NR-V2X network based on its local knowledge.

C. CH-RRI SPS DESCRIPTION

This subsection discusses in detail the proposed Ch-RRI SPS protocol. As shown in Fig. 4, Ch-RRI SPS makes significant enhancements to the conventional SPS algorithm. The green boxes represent the steps of the Ch-RRI algorithm and all other steps are from the conventional SPS.

- **RRI Initialization and Sensing (Steps 1-2):** Similar to SPS, Ch-RRI SPS continuously measures the RSRP and S-RSSI of the previous $N_{sensing}$ slots and stores

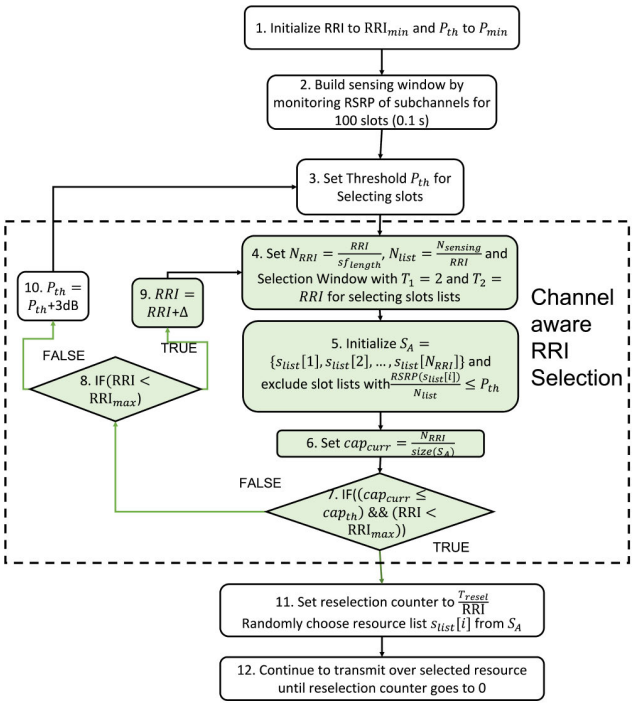

FIGURE 4. Flowchart of Ch-RRI SPS.

the sensing measurements in the sensing window (Step 1). In Step 2, Ch-RRI initializes the estimated $\widehat{\text{RRI}}$ to RRI$_{min}$ and the the RSRP threshold (P_{th}) to a minimum value P_{min}. The selection window in Ch-RRI SPS is not initialized before the resource selection process has started (see Step 2 in Fig. 2), and as available resources are identified and the estimated $\widehat{\text{RRI}}$ is changed, the selection window is updated. As in SPS, Ch-RRI SPS sets and updates the P_{th} (See Step 3).

- **Ch-RRI: Channel-aware RRI Selection (Steps 4-10):** Each vehicle utilizes $N_{sensing}$ slots (obtained in Step 2) for identifying the available slots and subsequently, selecting the minimum RRI possible in between transmission while ensuring that there remain resources (or slots) for other vehicles.
  1) In Step 4, Ch-RRI updates the estimated $\widehat{\text{RRI}}$ and initializes the selection window with $T_1 = 1$ and $T_2 = \widehat{\text{RRI}}$. T_1 is fixed to 1 to maximize slot resources.
  2) Each vehicle populates set S_A with all slots in the selection window and S_B as an empty set (See Step 5). The candidate slot exclusion criteria is also borrowed from SPS, except that, $\widehat{RRI}$ is an adjustable parameter in Ch-RRI.
  3) If the number remaining slots in S_A is less than 20% of the total available slots (Step 7), then, Ch-RRI, unlike SPS, first checks whether the $\widehat{\text{RRI}} <$ RRI$_{max}$ (Step 8). If yes, $\widehat{\text{RRI}}$ is increased by Δ as shown in Step 9, and Steps 4 - 7 are repeated. Once $\widehat{\text{RRI}}$ has reached RRI$_{max}$, then P_{th} is increased by 3 dB in Step 10, and Steps 3 - 7 are repeated.
- **Resource Selection** (Step 11) and **Resource Reselection** (Step 12) are similar to SPS. As in SPS, a reselection counter (RC) value is chosen such that the resource reservation is restricted between 0.5 and 1.5 s, irrespective of chosen $\widehat{\text{RRI}}$. However, in the case of Ch-RRI SPS, since RC is zero, unlike SPS (see Steps 8-9 in SPS flowchart), Ch-RRI SPS does not allow re-reservation of slot resources. Both these modifications are to ensure that Ch-RRI allows each vehicle to adjust its RRI at the time of resource reselection and account for changing vehicle traffic conditions.

V. AOI-RRI: AGE OF INFORMATION AWARE RRI SELECTION ALGORITHM

In this section, we provide some intuitions on the potential limitations of Ch-RRI, provide a brief background of Age-of-Information (AoI), and formulate the problem of AoI minimization in vehicular networks as an ILP problem. We discuss why the ILP formulation is impractical to solve for a decentralized network and propose AoI-RRI, a decentralized AoI-aware RRI selection algorithm.

A. LIMITATION OF CH-RRI ON COOPERATIVE AWARENESS

Though Ch-RRI is a promising RRI adaptation algorithm and promises to improves the cooperative awareness as discussed in Section IV, it has certain limitations as presented in this section.

- Ch-RRI SPS is based on the accurate knowledge of channel occupancy at any given time, however, given the dynamics of vehicles and channel usage, obtaining accurate channel availability information at each vehicle is not possible.
- Ch-RRI SPS attempts to enable each vehicle to transmit at the minimum RRI while accounting for 100% channel occupancy. However, the optimal trade-off between channel occupancy and optimal RRI may not be at 100 % channel occupancy.

Motivated by these limitations, we consider optimizing for a novel information freshness metric, namely AoI. Since optimizing for AoI guarantees freshness (and thus the best tracking error in this context), we can better account for trade-off between the optimal RRI and channel occupancy.

B. AGE OF INFORMATION

The AoI quantifies the *freshness* of information at any receiving node that was originally generated and transmitted by the transmitting node [28]. For the purposes of vehicular networks, AoI is the elapsed time since the last received location packet was generated at the transmitting vehicle. Let t^g denote the time that the packet containing the most recent location at sender vehicle u was generated. Assuming a linear cost function for the AoI evolution, the AoI at the receiving vehicle v assuming the current time is t is:

$$\text{AoI}_{uv}(t) = t - t^g. \tag{6}$$

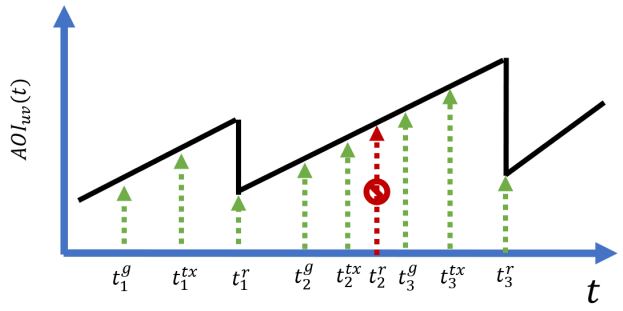

FIGURE 5. ***AoI*$_{uv}$ is the AoI at vehicle *v* based on the latest received transmission from vehicle *u*.**

The evolution of the AoI for vehicle v is illustrated in Fig. 5. The generation, transmission, and reception times of the i^{th} location packet are denoted by t_i^g, t_i^{tx}, and t_i^r. Therefore, the overall delay for a packet $= (t_i^r - t_i^g)$.

Eq. 6 can be used to find the average AoI_{uv} between vehicle v and neighboring vehicle u. The average AoI_{uv} is found by calculating the area under $\text{AoI}_{uv}(t)$. The area under $\text{AoI}_{uv}(t)$ is normalized by the observation time T_{obs} [28]

$$\text{AoI}_{uv} = \frac{1}{T_{obs}} \int_{T_{obs}} \text{AoI}_{uv}(t). \tag{7}$$

We represent the set of all vehicles in the environment as $\mathcal{N}$ and the set of all neighboring vehicles of v as $\mathcal{N}_v \subseteq \mathcal{N}$, where $u \in \mathcal{N}_v$. The average AoI at vehicle v is:

$$\text{AoI}_v = \frac{1}{|\mathcal{N}_v|} \sum_{u \in \mathcal{N}_v} \text{AoI}_{uv}. \tag{8}$$

The overall system AoI with $|\mathcal{N}|$ vehicles can be computed as:

$$\text{AoI} = \frac{1}{|\mathcal{N}||(\mathcal{N}-1)|} \sum_{v \in \mathcal{N}} \sum_{u \in \mathcal{N}_v} \text{AoI}_{uv}, \tag{9}$$

where $|\mathcal{N}||(\mathcal{N}-1)|$ are the number of unique pairs of sender and receivers in the system. Assuming the simple vehicular network in Fig. 1 with vehicles u and v, we can assume that inter-packet reception interval between receiver v and transmitter u are multiples of the RRI. Using these assumptions and the fact that the AoI resets to 0 upon successful reception of location information, the evolution of the AoI at the receiving vehicle can be written as

$$\text{AoI}(t + \text{RRI}) = \begin{cases} 0, & \text{if a packet is received} \\ \text{AoI}(t) + \text{RRI}, & \text{otherwise} \end{cases} \tag{10}$$

Note that Eq. 10 implies that minimizing the RRI also minimizes the AoI at the receiving vehicle. However, too many vehicles transmitting with a small RRI can increase the number of lost packets due to congestion, which also increases the AoI. Therefore, as in the case of tracking error, there is a tradeoff between smaller RRIs and improved AoI performance.

C. AOI ILP PROBLEM FORMULATION

The objective of AoI-RRI is to minimize the overall system AoI based on what each vehicle observes. As in the Ch-RRI problem formulation, finding an optimal RRI that minimizes the system AoI can be written as a Integer Linear Programming (ILP) problem.

1) OBJECTIVE FUNCTION

Eq. 11 is the objective function where each vehicle chooses a RRI at each vehicle v (where $v \in \mathcal{N}$) such that the AoI is minimized over the entire time duration T.

$$\sum_{t \in T} \frac{1}{|\mathcal{N}|} \sum_{u,v \in \mathcal{N}} \text{AoI}_{uv}(t). \tag{11}$$

$$\text{subject to } \text{RRI}_{min} \leq \text{RRI}_v(t) \leq \text{RRI}_{max}, \forall v \in \mathcal{N}, t \in T \tag{12}$$

2) CONSTRAINTS

Eq. 12 restricts the RRI for each vehicle to the range $[\text{RRI}_{min}, \text{RRI}_{max}]$. Note that there are no capacity constraints for Eq. 11, and the AoI minimization itself decides the optimal tradeoff.

However, as in the case of Eq. 3, solving Eq. 11 assumes global information at every vehicle and knowledge of each vehicles channel information and mobility even at future time instants, which is not realistic. As a result, this ILP is not practical. Thus we propose AoI-RRI, an algorithm that attempts to iteratively minimize the NR-V2X system AoI in a decentralized manner, described in Section V-D

D. AOI-RRI SPS

This section details AoI-RRI SPS, SPS powered by a decentralized AoI-aware RRI selection algorithm. AoI-RRI finds a RRI_v (where $\text{RRI}_v \in [\text{RRI}_{min}\ \text{RRI}_{max}]$) for vehicle v by iterating the previously chosen RRI, denoted RRI^{t-1}, such that the locally measured average AoI is minimized. The algorithm runs in three steps. First, at the RRI selection time, v uses the sensing window history to measure the channel congestion in the network. Second, v calculates the time since the last received packet from every vehicle in the vicinity to estimate the local average AoI, and adjusts its RRI in order to minimize this last measured AoI. Finally, v uses the semi-persistent scheduling procedure presented in Fig. 2 and selects slot resources using the latest selected RRI. The algorithm details are as follows:

1) STEP 1: SENSING AND CHANNEL CONGESTION DETECTION

In line 1 of Algorithm 1, AoI-RRI uses a channel congestion detection algorithm, further detailed in Algorithm 2, to measure and detect whether or not significant channel congestion has occurred. The channel congestion algorithm returns **true** if there is significant congestion detected and like Ch-RRI SPS, uses the previously chosen RRI^{t-1} and the RSRP sensing measurements for the last $N_{sensing}$ slots, i.e. the sensing window, as inputs. In line 2 of Algorithm 2,

v calculates the size of the set S_{total}, which is the set of all possible slots resources using RRI^{t-1}. Lines 3-5 of Algorithm 2 populate set S_{avail} with those slots with linear average RSRP measurements higher than P_{th}^{t-1}. If the number of slots in S_{avail} is less than 20% of the total available slots, it means that network congestion has increased since the previous resource reservation, and RRI^{t-1} or P_{th}^{t-1} must be increased. Using RSRP measurements can give a robust estimate of the channel congestion without adding any sensing overhead since the sensing window measurements and RSRP threshold are taken as a part of the SPS procedure. If the channel congestion increases, lines 2-3 of Algorithm 1 automatically increase the RRI to avoid congesting the channel further.

2) STEP 2: AOI ESTIMATION AND RRI ADJUSTMENT

If the channel has not become significantly congested, vehicle v uses Eqs. 6 and 8 and computes its local AoI by calculating and averaging the time since the last received packet from each neighboring vehicle. The AoI-RRI algorithm iterates upon the last chosen RRI to minimize the most recent average AoI at each vehicle v. AoI-RRI uses one of the following three actions– (1) **DECR** - decrease RRI, (2) **INCR** - increase RRI, and (3) **SAME** - maintain the same RRI.[7] Algorithm 1 presents the pseudocode for this step.

Lines 4-9 form the core of AoI-RRI where AoI_{avg} for the current and previous T_{obs} are compared. In lines 4-6 AoI-RRI checks if the local AoI has increased by a factor of more than σ_t, in which case the AoI has significantly worsened and AoI-RRI reverses the previously selected action. If in lines 7-9, v sees that the local AoI has decreased by a factor of more than σ_t, the previous action selected by the algorithm is repeated, i.e. the RRI continues to increase or decrease. If there is no significant change in AoI, AoI-RRI chooses the same RRI as before. Finally, in 10-20, the new RRI is calculated based on the action selected in lines 2-9. The new RRI returned is maintained until the end of the current T_{obs}. Further, β decides the magnitude by which the RRI changes if the chosen action was **INCR** or **DECR**.

3) STEP 3: SEMI-PERSISTENT SCHEDULING

Finally, v uses the RRI selected from Algorithm 1 to choose a slot for transmission using the SPS procedure presented in Fig. 2. Note that the P_{th} value that is used to select the slots is stored as a part of the procedure, and again the next time resources are selected.

VI. SIMULATION OVERVIEW AND RESULTS

In this section we cover the simulation settings, performance metrics, and compare the proposed Ch-RRI SPS and AoI-RRI SPS to static RRI SPS.

[7]The concept of utilizing these actions for adjusting the RRI is inspired by the algorithm presented in [38].

Algorithm 1 AoI-RRI Algorithm at Vehicle v

Input: RSRP of $N_{sensing}$ slots across J subchannels in sensing history, $s_{total} = [s_1^j, \cdots, s_{N_{sensing}}^j]$, Minimum Power threshold (P_{min}), Maximum Power threshold (P_{max}), RRI chosen during the previous T_{obs}, RRI^{t-1}, local average AoI of the previous T_{obs}, AoI_{avg}^{t-1}, Action chosen during the previous T_{obs}, α^{t-1}), Power threshold chosen during the previous T_{obs}, (P_{th}^{t-1})

Output: New RRI^t, slot s_v for node v, and number of retransmissions N_{resel}

1: $[\text{channel}_{\text{flag}}] = \text{channel}_{cong}(\text{RRI}^{t-1}, s_{total}, P_{th}^{t-1})$ ▷ Checks to see if channel is congested
2: **if** $\text{channel}_{\text{flag}}$ ==true **then**
3: $\boldsymbol{\alpha^t}$ =INCR
4: **if** $AoI_{avg}^t > AoI_{avg}^{t-1} + \sigma_t$ **then**
5: $\boldsymbol{\alpha^t} = \text{inverse}(\alpha^{t-1})$ ▷ Previous action caused AoI to worsen significantly, so inverse action
6: **else if** $AoI_{avg}^t < AoI_{avg}^{t-1} - \sigma_t$ **then**
7: $\boldsymbol{\alpha^t} = (\alpha^{t-1})$ ▷ Previous action caused AoI to get better so continue action
8: **else**
9: $\boldsymbol{\alpha^t}$ =SAME ▷ AoI has not significantly changed from previous value, so maintain same RRI
10: **if** $\boldsymbol{\alpha^t}$ == INCR **then**
11: **if** $\text{RRI}^{t-1} \geq \text{RRI}_{max}$ **then**
12: $\text{RRI}^t = \text{RRI}^{t-1}$ ▷ AoI has improved but RRI has hit maximum
13: **else**
14: $\text{RRI}^t = \beta\ \text{RRI}^{t-1}$
15: **else if** $\boldsymbol{\alpha^t}$ == DECR **then**
16: **if** $\text{RRI}^{t-1} \leq \text{RRI}_{min}$ **then**
17: $\text{RRI}^t = \text{RRI}^{t-1}$ ▷ AoI has improve but RRI has hit minimum
18: **else**
19: $\text{RRI}^t = \frac{1}{\beta}\ \text{RRI}^{t-1}$
20: **else if** $\boldsymbol{\alpha^t}$ == SAME **then**
21: $\text{RRI}^t = \text{RRI}^{t-1}$
22: return P_{th}, RRI^t

A. SIMULATION SETTING

We modified and enhanced a system-level simulator originally designed to model C-V2X Mode-4 [39] to model and compare AoI-RRI SPS, Ch-RRI SPS, and NR-V2X Mode-2 SPS with three different static RRIs. We use the 3GPP highway mobility models [7] for our simulation results.

In the highway mobility model, vehicles move along a six lane highway, with three lanes dedicated to each direction. The highway models assume the velocity of vehicles moving in the positive direction and negative direction are drawn from truncated Gaussian distributions with means of v_{avg} and $-v_{avg}$, respectively. The Gaussian distribution mean and variance values are assumed to be 19.44 m/s (70 km/hr) and 3.0 m/s, respectively. As each vehicle in each lane approaches

Algorithm 2 Channel Congestion

Input: All slots in sensing history, $s_{total}(1 : N_{sensing})$, Power threshold selected from previous slot selection (P_{th}^{t-1}), RRI selected from previous AoI scheduling instance, RRI^{t-1}
Output: Returns true if the channel is congested as compared to the previous RRI, and false otherwise

procedure $\text{channel}_{\text{cong}}(s_{total}(1 : N_{sensing}), P_{th}^{t-1}, \text{RRI}^{t-1})$
  $N_{\text{RRI}} = \text{floor}(\frac{N_{sensing}}{\text{RRI}^{t-1}} - 1)$
  $S_i^j = \frac{1}{N_{\text{RRI}}} \sum_{k=0}^{N_{RRI}} s_{1+i+k\cdot\text{RRI}^{t-1}}^j$
  $S_{\text{total}} = [S_0^j, S_1^j, \ldots, S_{\text{RRI}^{t-1}}^j]$
  if $S_i^j < P_{th}^{t-1}$ **then**
    $S_{\text{avail}} \leftarrow S_i^j$
  if $\frac{|S_{\text{avail}}|}{|S_{\text{total}}|} < 0.2$ **then**
    return **true** ▷ The value of P_{th} has not changed as compared to the previous slot selection, so the channel is not congested
  else
    return **false** ▷ The value of P_{th} needs to increase by 3 dB as compared to the previous slot selection, so the channel is congested

TABLE 2. Simulation Parameters.

Parameter	Value
Vehicle density	{20-160} veh/km
Road Length/Number of lanes/Lane width	2000 m/ 6 lanes/ 4 m
β	1.1
Reselection time	0.5 -1.5 s
Simulation time	25 seconds
Transmission Power	23 dBm
Transmission and Sensing Range	300 meters
Distribution of vehicle speeds	N(19.44 m/s, 3 m/s)
AoI-RRI/Ch-RRI RRI_{max}	100 ms
AoI-RRI/Ch-RRI RRI_{min}	20 ms
Packet Size	190 B
MCS Index	7
Number of trials	10
Initial RSRP threshold, P_{th}	-90 dBm

the length of the highway, the warp used in the model places the vehicle at the opposite end of the highway. All vehicles remain in the same lane for the duration of the simulation. Each vehicle's initial location along the highway follows a Poisson distribution.

For comprehensive analysis, we compare the performance of Ch-RRI SPS and AoI-RRI SPS against conventional NR-V2X Mode-2 SPS with three different static RRIs: 20 ms RRI, 50 ms RRI, and 100 ms RRI. The vehicle densities in the simulation range from 20 to 160 veh/km, and initial positions and velocities do not change across AoI-RRI SPS, Ch-RRI SPS, and NR-V2X SPS. All simulations used a 10 MHz system bandwidth, 25 second simulation time, and results were averaged over 10 trials. Table 2 summarizes the default values of the key simulation parameters for AoI-RRI SPS, Ch-RRI SPS, and NR-V2X SPS with static RRIs.

B. PERFORMANCE METRICS

This work uses the following three metrics to compare AoI-RRI SPS, Ch-RRI SPS, and static RRI SPS.

- **Tracking Error ($\mathbf{e_{track}}$)**- e_{track} is calculated as the difference in the transmitting vehicle u's actual location and estimated location from u's last received transmission at receiver vehicle v. (see Section III-A).
- **Age of Information (AoI)** - The difference in the reception time at receiver vehicle v of vehicle u's last location and the generation time of u's last location (see Section V-B).
- **Packet Delivery Ratio (PDR)** - The likelihood that all neighbors inside the transmission range of a vehicle successfully receive the transmitted packet. Formally, the PDR is computed as $\text{PDR}_u = \frac{PR_i}{PD_i}$. PD_i is the number of packets sent by vehicle i and PR_i is the number of packets received by neighboring vehicles originally transmitted by vehicle i.

C. EXPERIMENTAL RESULTS

1) AVERAGE TRACKING ERROR AND SYSTEM AOI

Figs. 6(a) and 6(b) compare the system tracking error and AoI, respectively, of AoI-RRI SPS and Ch-RRI SPS to 20 ms, 50 ms, and 100 ms static RRI SPS. Fig. 6 demonstrates that tracking error worsens with increasing density, with the 20 ms RRI SPS tracking error giving the best static RRI SPS performance. Both tracking error and AoI increase drastically at higher densities (larger than 100 veh/km). Since there are insufficient slot resources to support a 20 ms RRI without two vehicles in the same vicinity choosing the same slot resource, there are increased packet losses, leading to worse performance at high densities. The tracking error for AoI-RRI is smaller than the tracking error of Ch-RRI and all three static RRIs across large vehicle densities. AoI-RRI outperforms 20 ms RRI NR-V2X (the best performing fixed RRI) in terms of AoI by almost 19% and 16% respectively at 120 and 160 veh/km. This indicates that AoI-RRI finds for each vehicle a RRI that minimizes packet losses and enables timely cooperative awareness in the network. The AoI improvements found with AoI-RRI extend to the tracking error. AoI-RRI was also found to have an advantage over Ch-RRI in high density scenarios as well outperforming Ch-RRI at 120 and 160 veh/km by 9.16% and 10.81%, respectively. The tracking error results show that lower average RRIs aid vehicles in high and low density situations. Even in high density scenarios, (160 vehicles/km), both AoI-RRI and Ch-RRI outperform the 20 and 50 ms RRI.

2) RRI DISTRIBUTION

Figs. 7(a)-7(b) show the average RRI distributions for AoI-RRI and Ch-RRI for selected densities over the last five seconds of the simulation.[8] Across densities, AoI-RRI shows a larger RRI variance as compared to the Ch-RRI. This large variance in the RRI distribution for the AoI-RRI algorithm can be attributed to varying traffic densities and

[8]We use the last five seconds because by then, every vehicle has had sufficient time to choose an acceptable RRI and we can analyze steady state behavior.

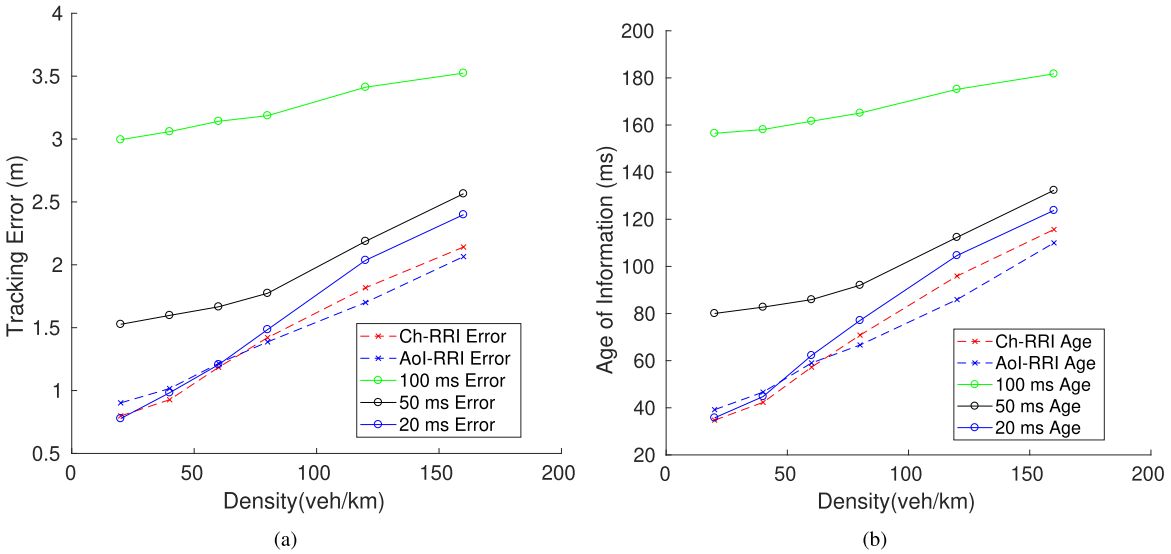

(a) (b)

FIGURE 6. (a) Average tracking error and (b) Average system age of information.

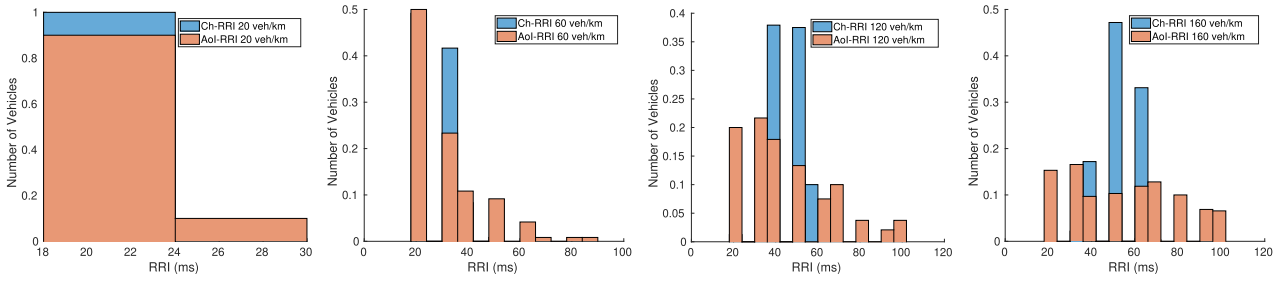

(a) 20 veh/km (b) 60 veh/km (c) 120 veh/km (d) 160 veh/km

FIGURE 7. RRI distribution during the last 5 seconds of simulations across vehicle densities for Ch-RRI and AoI-RRI.

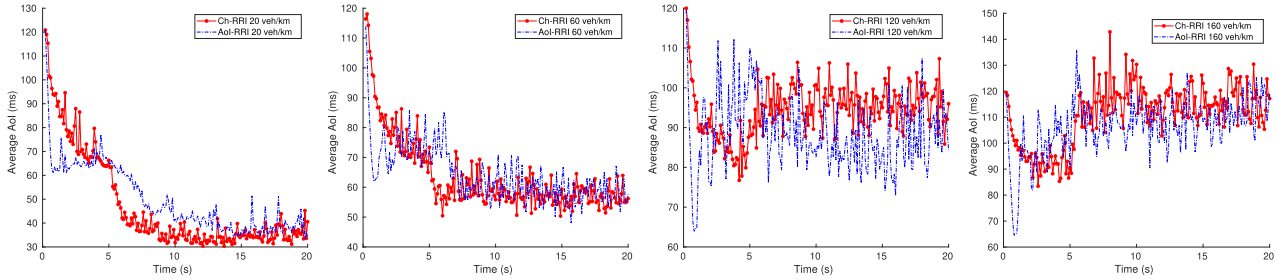

(a) 20 veh/km (b) 60 veh/km (c) 120 veh/km (d) 160 veh/km

FIGURE 8. Average AoI vs time across vehicle densities for Ch-RRI and AoI-RRI.

noisy estimates of the measured AoI which leads vehicles to choose different RRIs depending on the observed AoI. Although there is a large variance in the RRI distribution of the AoI-RRI, the AoI-RRI tracking error performance approaches that of Ch-RRI and 20 ms SPS for low densities, and outperforms all methods in high density scenarios. In Ch-RRI, the RRI distribution is comparatively narrow, and the average chosen RRI is similarly small for low densities (20 and 40 veh/km). This means that there are enough channel resources to support small RRIs for both Ch-RRI and AoI-RRI. In Fig. 7(b), we see that while the AoI-RRI RRI distribution skews towards RRI_{max}, many vehicles use lower RRIs, which contributes to the improved AoI performance.

We compare AoI-RRI, Ch-RRI, and static RRI SPS using the aforementioned tracking error, AoI, and PDR performance metrics. In addition to these metrics, we also look at the final RRI distributions and average AoI over time to better understand the operation of AoI-RRI and Ch-RRI.

3) AVERAGE AOI VS TIME

Figs. 8(a)-8(b) present the average AoI over simulation time of AoI-RRI SPS and Ch-RRI SPS. Both AoI-RRI and Ch-RRI

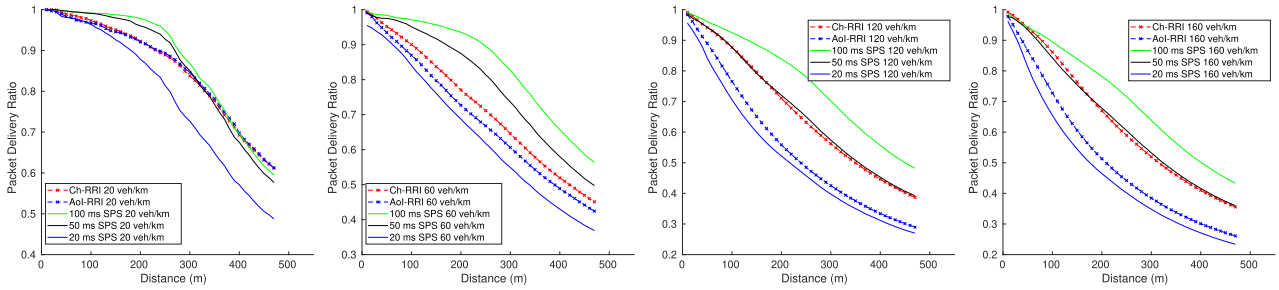

(a) 20 veh/km (b) 60 veh/km (c) 120 veh/km (d) 160 veh/km

FIGURE 9. PDR across vehicle densities.

algorithms start with an initial RRI of 50 ms, and only allow for adaptive RRIs to be chosen after 5 sec. This gives enough time for each algorithm to (i) allow all vehicles to transmit at least once and (ii) allow each algorithm to gather channel and AoI measurements. Notice that both AoI-RRI and Ch-RRI start with an initial value of 120 ms. This is because both algorithms start with observing the channel for 100 ms (following the NR-V2X Mode-2 SPS standard) before selecting an initial slot. Once both algorithms start transmitting, the AoI drops to 70 ms, which is expected for an RRI of 50 ms. In the low density cases (20 and 40 veh/km), both algorithms drop to average AoI of 40-50 ms. Note that Ch-RRI slightly outperforms AoI-RRI in lower densities. This is because Ch-RRI detects an empty channel and automatically transmits at the lowest possible RRI. Ch-RRI is also able to converge to a steady state value faster than AoI-RRI, likely because of the noisy nature of the AoI estimates. When the density increases, AoI-RRI is able to perform better, and is able to take actions that lead to a lower average AoI.

4) PACKET DELIVERY RATIO

Fig. 9 compares the AoI-RRI, Ch-RRI, and NR-V2X Mode-2 SPS PDRs across vehicle densities. Among the fixed RRI results, the 100 ms RRI performs the best, but correspondingly yield a large tracking error and AoI. Similarly, 100 ms RRI NR-V2X gives the worst PDR performance, but gave the best tracking error and AoI performance, meaning there is a tradeoff between PDR and RRI, that affects AoI performance. Both AoI-RRI and Ch-RRI attempt to find the best RRI that optimizes the tracking error and AoI.

Notice that at low densities (20 and 60 veh/km), the PDR of AoI-RRI and Ch-RRI are similar, as are the average AoI and tracking error. Both AoI-RRI and Ch-RRI choose similar RRIs and are able to achieve the best tracking error performance. As the densities increase the RRI distribution of AoI-RRI tends towards lower RRIs, and the PDR performance is worse than that of Ch-RRI, which chooses a larger average RRI. This indicates that the AoI-RRI finds that choosing a slightly lower RRI distribution can minimize the AoI, as the average age of AoI-RRI is lower than Ch-RRI. However, AoI-RRI does not select a 20 ms RRI for all vehicular since the AoI results show there are diminishing returns for selecting a low RRI, and eventually the increased congestion and packet collisions will deteriorate AoI and tracking error.

5) DISCUSSION

Unlike conventional SPS and Ch-RRI, the proposed AoI aware SPS is able to successfully learn the system AoI and adapt each vehicle's RRI across time-varying NR-V2X scenarios. As a result of choosing an optimal RRI, it is shown that the average tracking error of every vehicle pair is also reduced. This significantly improves the cooperative awareness of vehicular networks.

VII. CONCLUSION

In this work, we proposed two adaptive RRI algorithms to power SPS for improved cooperative awareness performance of decentralized V2X networks. Ch-RRI and AoI-RRI choose RRIs based on the availability of channel resources and measured AoI, respectively, and then use SPS for the selection of suitable BSM transmission opportunities at those chosen RRIs. Our extensive experiments based on NR-V2X Mode-2 standard demonstrated that SPS powered by either algorithm significantly outperforms conventional SPS in terms of the cooperative awareness performance in all considered NR-V2X scenarios. In the future, we will explore using nonlinear age functions and designing reinforcement learning (RL) based scheduling protocols that can learn vehicle priorities and other contextual factors over time.

REFERENCES

[1] K. Z. Ghafoor, L. Kong, S. Zeadally, A. S. Sadiq, G. Epiphaniou, M. Hammoudeh, A. K. Bashir, and S. Mumtaz, "Millimeter-wave communication for Internet of Vehicles: Status, challenges, and perspectives," *IEEE Internet Things J.*, vol. 7, no. 9, pp. 8525–8546, Sep. 2020.

[2] G. Thandavarayan, M. Sepulcre, and J. Gozalvez, "Analysis of message generation rules for collective perception in connected and automated driving," in *Proc. IEEE Intell. Vehicles Symp. (IV)*, Jun. 2019, pp. 134–139.

[3] S.-W. Kim, W. Liu, M. H. Ang, E. Frazzoli, and D. Rus, "The impact of cooperative perception on decision making and planning of autonomous vehicles," *IEEE Intell. Transp. Syst. Mag.*, vol. 7, no. 3, pp. 39–50, Fall 2015.

[4] G. Naik, B. Choudhury, and J.-M. Park, "IEEE 802.11bd & 5G NR V2X: Evolution of radio access technologies for V2X communications," *IEEE Access*, vol. 7, pp. 70169–70184, 2019.

[5] R. Molina-Masegosa, J. Gozalvez, and M. Sepulcre, "Comparison of IEEE 802.11p and LTE-V2X: An evaluation with periodic and aperiodic messages of constant and variable size," *IEEE Access*, vol. 8, pp. 121526–121548, 2020.

[6] R. Molina-Masegosa and J. Gozalvez, "LTE-V for sidelink 5G V2X vehicular communications: A new 5G technology for short-range vehicle-to-everything communications," *IEEE Veh. Technol. Mag.*, vol. 12, no. 4, pp. 30–39, Dec. 2017.

[7] M. H. C. Garcia, A. Molina-Galan, M. Boban, J. Gozalvez, B. Coll-Perales, T. Sahin, and A. Kousaridas, "A tutorial on 5G NR V2X communications," *IEEE Commun. Surveys Tuts.*, vol. 23, no. 3, pp. 1972–2026, 3rd Quart., 2021.

[8] *Intelligent Transport Systems (ITS); Vehicular Communications; Basic Set of Applications; Part 2: Specification of Cooperative Awareness Basic Service*, Standard ETSI EN 302 637-2, Version 1.3.2, Nov. 2014.

[9] V. Milanés, S. E. Shladover, J. Spring, C. Nowakowski, H. Kawazoe, and M. Nakamura, "Cooperative adaptive cruise control in real traffic situations," *IEEE Trans. Intell. Transp. Syst.*, vol. 15, no. 1, pp. 296–305, Feb. 2014.

[10] C.-L. Huang, Y. P. Fallah, R. Sengupta, and H. Krishnan, "Adaptive intervehicle communication control for cooperative safety systems," *IEEE Netw.*, vol. 24, no. 1, pp. 6–13, Jan. 2010.

[11] A. Rasouli and J. K. Tsotsos, "Autonomous vehicles that interact with pedestrians: A survey of theory and practice," *IEEE Trans. Intell. Transp. Syst.*, vol. 21, no. 3, pp. 900–918, Mar. 2020.

[12] B. Choudhury, V. K. Shah, A. Dayal, and J. H. Reed, "Experimental analysis of safety application reliability in V2V networks," in *Proc. IEEE 91st Veh. Technol. Conf. (VTC-Spring)*, May 2020, pp. 1–5.

[13] A. Dayal, V. K. Shah, B. Choudhury, V. Marojevic, C. Dietrich, and J. H. Reed, "Adaptive semi-persistent scheduling for enhanced on-road safety in decentralized V2X networks," in *Proc. IFIP Netw. Conf. (IFIP Networking)*, Jun. 2021, pp. 1–9.

[14] A. Dayal, "Practical algorithms and analysis for next-generation decentralized vehicular network," Ph.D. thesis, Bradley Dept. Elect. Comput. Eng., Virginia Tech, Blacksburg, Virginia, 2021.

[15] S. Chen, J. Hu, Y. Shi, and L. Zhao, "LTE-V: A TD-LTE-based V2X solution for future vehicular network," *IEEE Internet Things J.*, vol. 3, no. 6, pp. 997–1005, Dec. 2016.

[16] A. Nabil, K. Kaur, C. Dietrich, and V. Marojevic, "Performance analysis of sensing-based semi-persistent scheduling in C-V2X networks," in *Proc. IEEE 88th Veh. Technol. Conf. (VTC-Fall)*, Aug. 2018, pp. 1–5.

[17] A. Bazzi, G. Cecchini, A. Zanella, and B. M. Masini, "Study of the impact of PHY and MAC parameters in 3GPP C-V2V mode 4," *IEEE Access*, vol. 6, pp. 71685–71698, 2018.

[18] X. He, J. Lv, J. Zhao, X. Hou, and T. Luo, "Design and analysis of a short-term sensing-based resource selection scheme for C-V2X networks," *IEEE Internet Things J.*, vol. 7, no. 11, pp. 11209–11222, Nov. 2020.

[19] A. Bazzi, "Congestion control mechanisms in IEEE 802.11p and sidelink C-V2X," in *Proc. 53rd Asilomar Conf. Signals, Syst., Comput.*, Nov. 2019, pp. 1125–1130.

[20] F. Peng, Z. Jiang, S. Zhang, and S. Xu, "Age of information optimized MAC in V2X sidelink via piggyback-based collaboration," *IEEE Trans. Wireless Commun.*, vol. 20, no. 1, pp. 607–622, Jan. 2021.

[21] M. Bezmenov, Z. Utkovski, K. Sambale, and S. Stanczak, "Semi-persistent scheduling with single shot transmissions for aperiodic traffic," in *Proc. IEEE 93rd Veh. Technol. Conf. (VTC-Spring)*, Apr. 2021, pp. 1–7.

[22] M. Gonzalez-Martín, M. Sepulcre, R. Molina-Masegosa, and J. Gozalvez, "Analytical models of the performance of C-V2X mode 4 vehicular communications," *IEEE Trans. Veh. Technol.*, vol. 68, no. 2, pp. 1155–1166, Feb. 2019.

[23] C. Campolo, A. Molinaro, F. Romeo, A. Bazzi, and A. O. Berthet, "5G NR V2X: On the impact of a flexible numerology on the autonomous sidelink mode," in *Proc. IEEE 2nd 5G World Forum (5GWF)*, Antonella Molinaro, France, Sep. 2019, pp. 102–107.

[24] Z. Ali, S. Lagén, L. Giupponi, and R. Rouil, "3GPP NR V2X mode 2: Overview, models and system-level evaluation," *IEEE Access*, vol. 9, pp. 89554–89579, 2021.

[25] S. Bartoletti, B. M. Masini, V. Martinez, I. Sarris, and A. Bazzi, "Impact of the generation interval on the performance of sidelink C-V2X autonomous mode," *IEEE Access*, vol. 9, pp. 35121–35135, 2021.

[26] V. Todisco, S. Bartoletti, C. Campolo, A. Molinaro, A. O. Berthet, and A. Bazzi, "Performance analysis of sidelink 5G-V2X mode 2 through an open-source simulator," *IEEE Access*, vol. 9, pp. 145648–145661, 2021.

[27] T.-H. Lee and C.-F. Lin, "Reducing collision probability in sensing-based SPS algorithm for V2X sidelink communications," in *Proc. IEEE REGION 10 Conf. (TENCON)*, Nov. 2020, pp. 303–308.

[28] S. Kaul, R. Yates, and M. Gruteser, "Real-time status: How often should one update?" in *Proc. IEEE INFOCOM*, Mar. 2012, pp. 2731–2735.

[29] A. Baiocchi and I. Turcanu, "Age of information of one-hop broadcast communications in a CSMA network," *IEEE Commun. Lett.*, vol. 25, no. 1, pp. 294–298, Jan. 2021.

[30] A. Vinel, L. Lan, and N. Lyamin, "Vehicle-to-vehicle communication in C-ACC/platooning scenarios," *IEEE Commun. Mag.*, vol. 53, no. 8, pp. 192–197, Aug. 2015.

[31] N. Lyamin, B. Bellalta, and A. Vinel, "Age-of-information-aware decentralized congestion control in VANETs," *IEEE Netw. Lett.*, vol. 2, no. 1, pp. 33–37, Mar. 2020.

[32] R. D. Yates and S. K. Kaul, "The age of information: Real-time status updating by multiple sources," *IEEE Trans. Inf. Theory*, vol. 65, no. 3, pp. 1807–1827, Mar. 2019.

[33] A. Kosta, N. Pappas, A. Ephremides, and V. Angelakis, "Age of information performance of multiaccess strategies with packet management," *J. Commun. Netw.*, vol. 21, no. 3, pp. 244–255, Jun. 2019.

[34] A. Maatouk, M. Assaad, and A. Ephremides, "On the age of information in a CSMA environment," *IEEE/ACM Trans. Netw.*, vol. 28, no. 2, pp. 818–831, Apr. 2020.

[35] L. Cao, H. Yin, R. Wei, and L. Zhang, "Optimize semi-persistent scheduling in NR-V2X: An age-of-information perspective," in *Proc. IEEE Wireless Commun. Netw. Conf. (WCNC)*, Apr. 2022, pp. 2053–2058.

[36] A. Rolich, I. Turcanu, A. Vinel, and A. Baiocchi, "Impact of persistence on the age of information in 5G NR-V2X sidelink communications," in *Proc. 21st Medit. Commun. Comput. Netw. Conf. (MedComNet)*, Jun. 2023, pp. 15–24.

[37] S. Gyawali, S. Xu, Y. Qian, and R. Q. Hu, "Challenges and solutions for cellular based V2X communications," *IEEE Commun. Surveys Tuts.*, vol. 23, no. 1, pp. 222–255, 1st Quart., 2021.

[38] S. Kaul, M. Gruteser, V. Rai, and J. Kenney, "Minimizing age of information in vehicular networks," in *Proc. 8th Annu. IEEE Commun. Soc. Conf. Sensor, Mesh Ad Hoc Commun. Netw.*, Jun. 2011, pp. 350–358.

[39] G. Cecchini, A. Bazzi, B. M. Masini, and A. Zanella, "LTEV2Vsim: An LTE-V2V simulator for the investigation of resource allocation for cooperative awareness," in *Proc. 5th IEEE Int. Conf. Models Technol. Intell. Transp. Syst. (MT-ITS)*, Jun. 2017, pp. 80–85.

AVIK DAYAL (Member, IEEE) received the B.S. degree in electrical engineering from the University of Virginia, in 2011, and the M.S. and Ph.D. degrees in electrical engineering from Virginia Tech, in 2016 and 2021, respectively.

After the Ph.D. degree, he became a Senior Engineer with the Johns Hopkins Applied Physics Laboratory. His current research interests include distributed sensing systems, vehicular communications, stochastic geometry, and signal processing for radars and communications.

VIJAY K. SHAH (Member, IEEE) is currently an Assistant Professor with the Cybersecurity Engineering Department, College of Engineering and Computing, George Mason University, VA, USA, and he serves as the Director of the NextG Wireless Laboratory. His research interests include next-generation wireless communications and networking, particularly, 5G/6G cellular networks, open radio access networks (O-RAN), AI/ML, and spectrum sharing.

HARPREET S. DHILLON (Fellow, IEEE) received the B.Tech. degree in electronics and communication engineering from IIT Guwahati, in 2008, the M.S. degree in electrical engineering from Virginia Tech, in 2010, and the Ph.D. degree in electrical engineering from The University of Texas at Austin, in 2013.

After serving as a Viterbi Postdoctoral Fellow with the University of Southern California for a year, he joined Virginia Tech, in 2014, where he is currently a Professor in electrical and computer engineering, the Chair of the Communications Area, the Associate Director of the Wireless@VT Research Group, and the Elizabeth and James E. Turner Jr. '56 Faculty Fellow. His research interests include communication theory, wireless networks, geolocation, and stochastic geometry. He is a fellow of AAIA and a Clarivate Analytics (Web of Science) Highly Cited Researcher. He has received six best paper awards, including the 2014 IEEE Leonard G. Abraham Prize, the 2015 IEEE ComSoc Young Author Best Paper Award, and the 2016 IEEE Heinrich Hertz Award. He has also received Early Achievement Awards from three IEEE ComSoc Technical Committees, namely the Communication Theory Technical Committee (CTTC), in 2020, the Radio Communications Committee (RCC), in 2020, and the Wireless Communications Technical Committee (WTC), in 2021. He was named the 2017 Outstanding New Assistant Professor, the 2018 Steven O. Lane Junior Faculty Fellow, the 2018 College of Engineering Faculty Fellow, and a recipient of the 2020 Dean's Award for Excellence in Research by Virginia Tech. His other academic honors include the 2008 Agilent Engineering and Technology Award, the UT Austin MCD Fellowship, the 2013 UT Austin WNCG Leadership Award, and the Inaugural IIT Guwahati Young Alumni Achiever Award 2020. He has served as the TPC Co-Chair for IEEE WCNC 2022 and the symposium TPC co-chair for many IEEE conferences. He has also served on the editorial boards of several IEEE journals with his current appointments being on the Executive Editorial Committee for IEEE TRANSACTIONS ON WIRELESS COMMUNICATIONS and a Senior Editor for IEEE WIRELESS COMMUNICATIONS LETTERS.

JEFFREY H. REED (Life Fellow, IEEE) is currently the Founder of Wireless @ Virginia Tech, where he also served as the Director, until 2014. He is the founding Faculty Member of the Ted and Karyn Hume Center for National Security and Technology and served as its Interim Director when founded, in 2010. He has published the book, *Software Radio: A Modern Approach to Radio Design* (Prentice Hall) and his latest textbook *Cellular Communications: A Comprehensive and Practical Guide* (Wiley-IEEE, 2014). He is the Co-Founder of Cognitive Radio Technologies (CRT), a company commercializing of the cognitive radio technologies; Federated Wireless, a company developing spectrum sharing technologies; and PFP Cybersecurity, a company specializing in security for embedded systems. In 2005, he became a fellow to the IEEE for contributions to software radio and communications signal processing and for leadership in engineering education. In 2013, he was awarded the International Achievement Award by the Wireless Innovations Forum. In 2012, he served on the President's Council of Advisors of Science and Technology Advisory Group that examined ways to transition federal spectrum for commercial use. He is a past member of CSMAC, a group that provides advice to the NTIA on spectrum issues.